Revue Roumaine de Chimie, **2009**, *54*(5), 389–397

A STUDY ON PROPERTIES OF THE POLYMERIC COMPOSITES BASED ON TRIAZENE POLYACRYLATES AND SILICATES

Lenuța STROEA and Emil C. BURUIANĂ*

"Petru Poni" Institute of Macromolecular Chemistry, 41 A Gr. Ghica Vodă Alley, 700487, Iaşi, Roumania

Received September 26, 2008

A new type of hybrid materials with montmorillonite and triazene polyacrylates as poly [(1-(phenyl)-3-(2 acryloyloxyethyl)-3-methyl triazene-1-co-methyl methacrylate] (**PAT_1**) and poly [1-(*para* chloro-phenyl)-3-(2 acryloyloxyethyl)-3-methyl triazene-1-co-methyl methacrylate] (**PAT_2**)) has been successfully prepared using the solution-intercalation film-casting technique. The nanoscale silicate layers are intercalated in the polyacrylates matrix as resulted by X-ray diffraction (XRD) and scanning electron microscopy (SEM). Additional information regarding the structure of triazene polyacrylates nanocomposites (**PAT_1/MMT** and **PAT_2/MMT**) were obtained by FT-IR analysis, atomic force microscopy (AFM) and thermal decomposition behavior, the latter indicating a higher thermal stability compared to the starting triazene copolymers.

INTRODUCTION

Nanocomposites consisting of organic polymers and inorganic nanoparticles are a new class of materials that may combine new and superior properties compared to corresponding micro- and macro-composites and to unfilled polymers. Due to the unique interfacial properties and phase morphology at the nanometer scale, nanocomposites exhibit enhanced physical and chemical properties as compared to their pure polymers. Moreover, such improvement is obtained without the increase of polymer density and the loss of its optical properties[1] and this can include, for example, increased moduli, better mechanical and thermal properties,[2-5] lower gas permeability,[6,7] higher fire retardation capability[1] and advanced surface hardness. Generally, all these progresses can be obtained at a very low silicate loading, usually below 5 wt %. For a better understanding of all the aspects, in the past decade numerous studies were reported in which intensive research interest was focused to evidence the potential applications of materials in tough and heat-resistant materials,[8] coatings,[9] electronics,[9] catalysis,[10] etc.

Depending on the nature of the components and the method of preparation, two broad classes of polymer silicate nanocomposites (intercalated and exfoliated) may be obtained. In the intercalated nanocomposites, the polymer chains penetrate into the galleries between the silicate layers, resulting in a well ordered multilayer morphology built up with alternating polymeric and inorganic layers. In the case of exfoliated or delaminated nanocomposites, all the silicate layers are delaminated into single layers and they are completely and uniformly dispersed in a continuous polymeric matrix. The silicate content of an exfoliated nanocomposite is usually lower than that in an intercalated nanocomposite, but in practice is often observed a combination of these two.

Montmorillonite, hectorite and saponite are the commonly used layered silicates. Among them, montmorillonite (MMT), a 2:1 layered silicate with lamellar shape, became the most employed in the preparation of polymer/clay nanocomposites. Classically, the chemical structure of MMT consists of two fused silica tetrahedral sheets sandwiching an edge-shared aluminum or magnesium octahedron sheet. The Na^+ and Ca^{2+} from the interlayer galleries can be replaced by organic cations such as alkylammonium ions via a cationic-exchange reaction to provide the hydrophobic layered silicate. In the literature, most of the nanocomposite materials are based on linear polymers like polyimide,[11-13] polyolefins,[14] polystyrene,[15] polyurethanes,[16] polyacrylates,[17,18] etc.

* Corresponding author: emilbur@icmpp.ro

We have to mention that previously, our group approached and developed a variety of novel polyacrylates[19-22] with triazene group (-N=N-N-) on the backbone intended for versatile applications. Furthermore, the synthesis of new triazene polymers seems to be of great importance because they can combine the sensitivity of the triazene structure with the properties of the resulting polymers in order to create new materials for microlithography. In this context, the broad spectrum of applications of the polymeric nanocomposites, determined us to prepare and characterize organoclay-acrylic nanocomposite. Consequently, the correlations between the structure and properties of prepared triazene polyacrylates/MMT nanocomposites will be discussed comparatively with the corresponding starting polymers.

EXPERIMENTAL SECTION

1. Materials

MMT powder with a cationic exchange capacity (CEC) of 95 mEq/100 g was adopted as the inorganic component of hybrid composites. All materials used in the study were purchased from Sigma Aldrich Chemical Co. and used without further purification.

2. Preparation of Organophilic Montmorillonite

A suspension of MMT (5 g) was gradually added to an aqueous solution of dodecyl amine (2.2 g) and HCl 37% (1.2 mL) previously heated at 80 °C. The resulting mixture was vigorously stirred for 6 hours at 80 ºC. The intercalating agent needed for the cation-exchange reaction was added 1.2 times in excess of MMT. A white solid product formed after filtration was collected and repeatedly washed with deionized water and acetone. The wet clay was dried at 100 °C for 12 h and as a final point, the modified montmorillonite was ground to powdery state.

3. Preparation of Triazene Acrylic Copolymers

The general structure of triazene polyacrylates, 1-(phenyl)-3-(2 acryloyloxyethyl)-3-methyl triazene-1-co-methyl methacrylate (**PAT_1**) and 1-(*para* chloro-phenyl)-3-(2 acryloyloxyethyl)-3-methyl triazene-1-co-methyl methacrylate (**PAT_2**) employed in our study is presented in Scheme 1.

The synthetic details for the triazene acrylic copolymers were discussed in details elsewhere.[21,22] Polyacrylates with triazene group in the side chain (-N=N-N-) are prepared by free radical copolymerization between the triazene monomers and methyl methacrylate (MMA). The resulting copolymers were precipitated in methanol and dried for 48 h under reduced pressure.

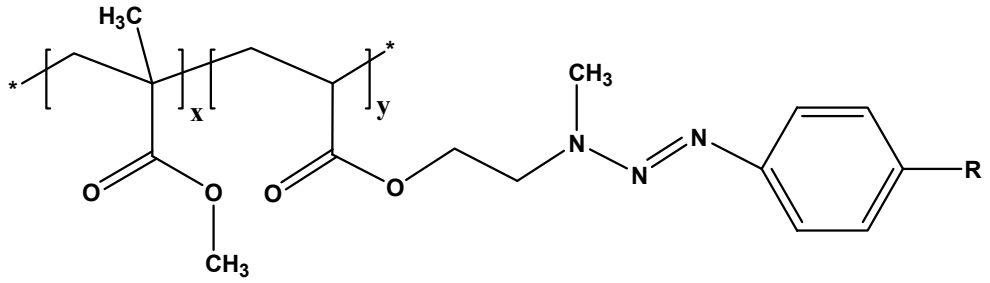

When R = H (PAT_1)
R = Cl (PAT_2)

Scheme 1 – The structure of triazene polyacrylates (PAT_1 and PAT_2).

4. Preparation of Triazene Polyacrylates/Clay Nanocomposite Films

Nanocomposites were prepared by using the solution-intercalation film-casting technique. For each composition, 1 g of triazene acrylic polymer was dissolved in 10 mL of dimethylformamide (DMF). Clay dispersions (3 wt %) were obtained by suspending a well-dried clay in DMF in a separate beaker. Both the polyacrylates solution and clay suspension were sonicated separately for 20 min with an Ultrasonic Processor GEX-500 probe sonicator at 21 W and room temperature and subsequently mixed. The final mixture was further sonicated for 10 min. The mixture was then cast on a glass surface and kept in a desiccator for controlled evaporation of the solvent over 2 days, and then the resulting nanocomposite (**PAT_1/MMT and PAT_2/MMT)** films were dried at 80 °C again in vacuum.

CHARACTERIZATION

The polymer structures were verified by ^{1}H-NMR, FTIR and UV spectroscopy using a Bruker 400-MHz spectrometer with tetramethylsilane as an internal standard, a Bruker Vertex 70 and a Specord M42 spectrophotometer, respectively. The thermal stability of triazene polyacrylates was analyzed through thermogravimetry using a MOM Budapest derivatograph. TGA thermograms were recorded between 0 °C and 750 ºC with a heating rate of 10 ºC min^{-1} in air. A SOLVER PRO-M atomic force microscope was used to probe the

surface morphology. The film thickness was determined with an interferential microscope (Linnik). An X-ray diffractometer (XRD, Bruker Advance D8) was used to examine ordering in clay and triazene polyacrylates/clay nanocomposites. Data were obtained in the 2θ range of 2-10° at a scan rate of 1.8°/min. SEM images were obtained on a ABT-60 scanning electron microscope (Topcon).

RESULTS AND DISCUSSON

1. Synthesis of Triazene Acrylic Copolymers

Detailed synthesis of triazene acrylic copolymers (PAT_1 and PAT_2) was discussed elsewhere.[21,22] Both polymers present a high solubility in common solvents such as DMF, DMSO, chloroform, and dichloromethane, and have film-forming properties. All the spectral data of these photopolymers are listed in Table 1 and as an example in Fig. 1, is presented the ^{1}H-NMR spectrum of the first triazene acrylic copolymer (PAT_1).

In this case, the most interesting peaks are those assigned to the aromatic protons located at 7.4 and 7.1 ppm, and the aliphatic ones from the spectral zone of 2.2–0.7 ppm because these signals can be used to calculate the copolymer composition. Taking in consideration the ratio of the integral peak for the aforementioned signals, it was determined the copolymer composition in the case of PAT_1 (the molar fraction of the triazene monomer was 0.24) and PAT_2, respectively, where the molar fraction of the corresponding monomer was 0.11.

Table 1

^{1}H-NMR spectral data for the synthesized triazene acrylic copolymers in chloroform

Sample	Chemical shifts (ppm)				
	$\delta_{aromatic}$	$\delta_{\underline{CH}2\text{-}\underline{CH}2}$	$\delta_{\underline{CH}3\text{-}O\text{-}C=0}$	$\delta_{\underline{CH}3\text{-}N=N\text{-}N}$	$\delta_{aliphatic\ from\ the\ acrylic\ backbone}$
PAT_1	7.1-7.4	4.4-3.7	3.6	3.34	2.2-0.7
PAT_2	7.33	4.4-4.0	3.6	3.2	2.0-0.7

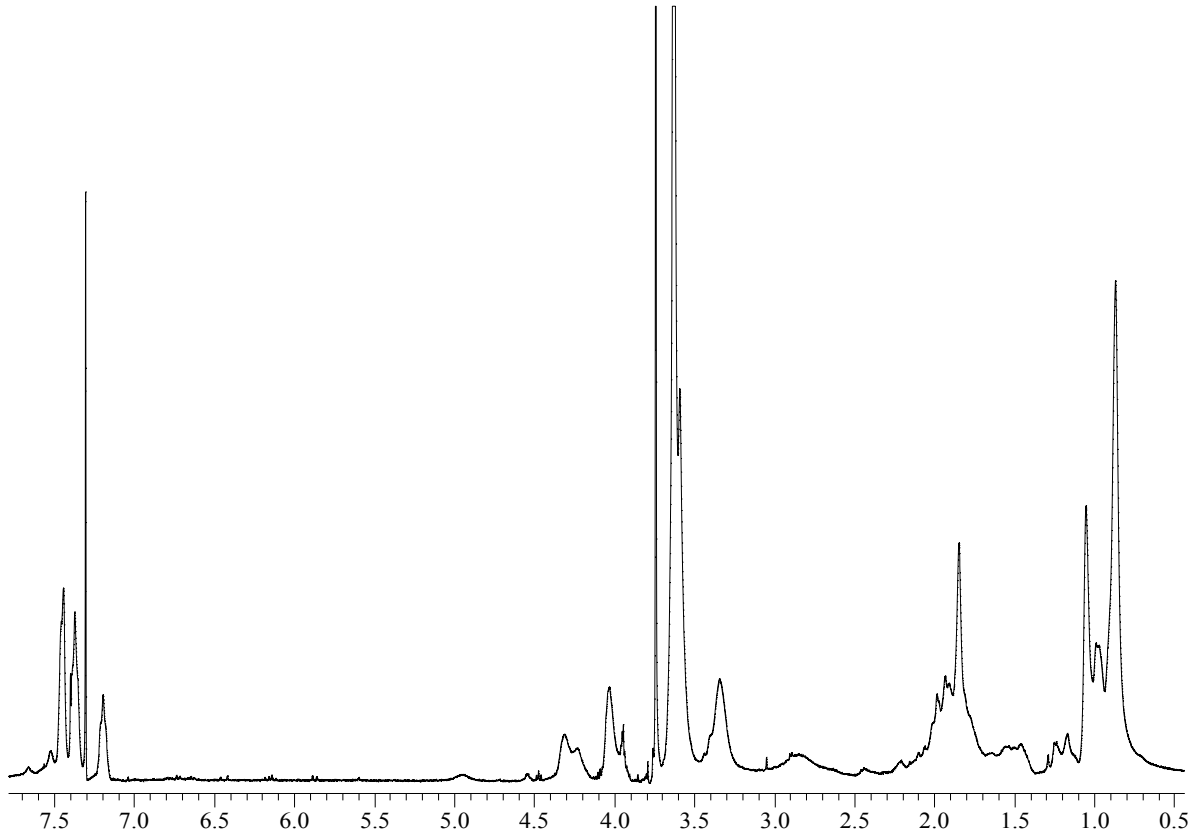

Fig. 1 – ^{1}H-NMR spectrum of 1-(phenyl)-3-(2 acryloyloxyethyl)-3-methyl triazene-1-co-methyl methacrylate (**PAT_1**) in $CDCl_3$.

In the IR spectra (not shown here), the triazene acrylic copolymers display the same absorption bands like in the starting monomers, not including the stretching vibration of the C=C double bond, which confirms the copolymerization of monomeric units. Characteristic of the triazene structure chemically anchored to the polymeric chain is the absorption at 1375 cm^{-1}.

2. Functionalization of MMT by dodecyl amine

Surface modification of organoclays being the most important step to achieve polymer nanocomposites, MMT was the subject of an organic treatment with dodecyl amine/HCl to become hydrophobic, and to guarantee a perfect compatibility or chemical bonding with polymers. Therefore, MMT, a hydrophilic clay containing stacked silicate sheets, can exchange the interlayer inorganic cations (e.g., Na^{+}, Ca^{2+}) with organic quaternary ammonium cations and through this reaction, the long alkyl chains of quaternary ammonium cations can be interpenetrated into the MMT clay galleries reducing the layer–layer attraction. Both the enlarged spacing and organophilic nature of the alkyl chains in ammonium cations would facilitate a favorable diffusion and accommodation of polymer or precursor into the interlayer space. The crystal structure of MMT consists of two-dimensional layers formed by fusing two silica tetrahedral sheets to an edge-shared octahedral sheet of aluminum hydroxide.

Fig. 2 shows typical XRD patterns of native and modified MMT, where the silicate layer (001) reflection has peak at 2θ = 5.94° for original MMT and 2θ = 5° for the organo-modified MMT, respectively.

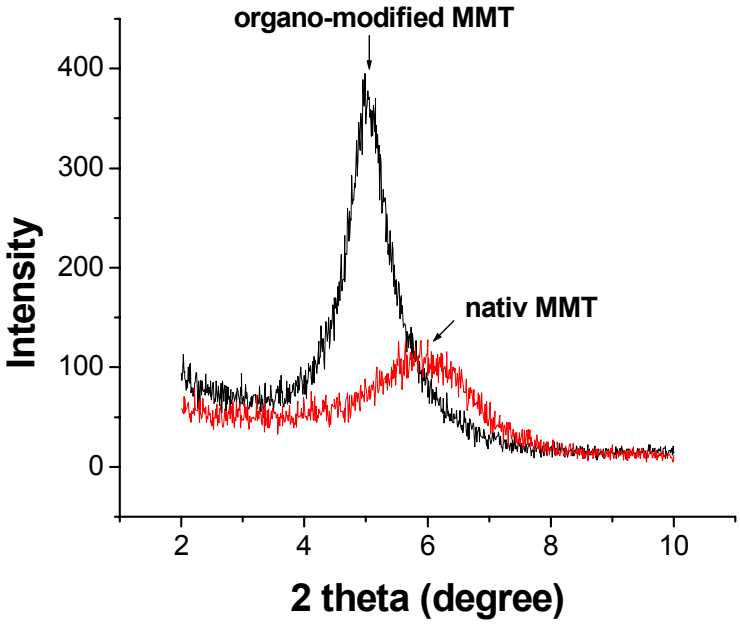

Fig. 2 – XRD patterns of native MMT and organo-modified MMT.

The d_{001} spacing was calculated from peak positions using Bragg's law:

$$d = \frac{\lambda}{2 \sin\theta}$$

where λ corresponds to the wavelength of the X-ray radiation used in the diffraction experiment (in our case is 5.402 Å), d is the spacing between diffractional lattice planes and θ is the measured diffraction angle from the X-ray diffractograms. The interlamellar spacing was found to increase from 2.6 nm for untreated MMT to 3.1 nm after treatment with dodecyl amine, proving the presence of the intercalated agent into the MMT galleries with the considerably enlargement of the interlayer spacing.

3. Characterization of Triazene Polyacrylates-Clay Nanocomposites

Preparing of nanocomposites involved the dispersion of triazene acrylic copolymers in DMF

and after adding the desired amount of organo-modified MMT (3 wt %), the obtained suspension was sonicated with an ultrasonic processor.

XRD analysis is a powerful tool for examining the crystal structure and occasionally, for studying the process kinetics of polymer/clay nanocomposites[23]. Fig. 3 present the XRD peaks of the corresponding triazene acrylic/clay nanocomposites (**PAT_1/MMT and PAT_2/MMT**).

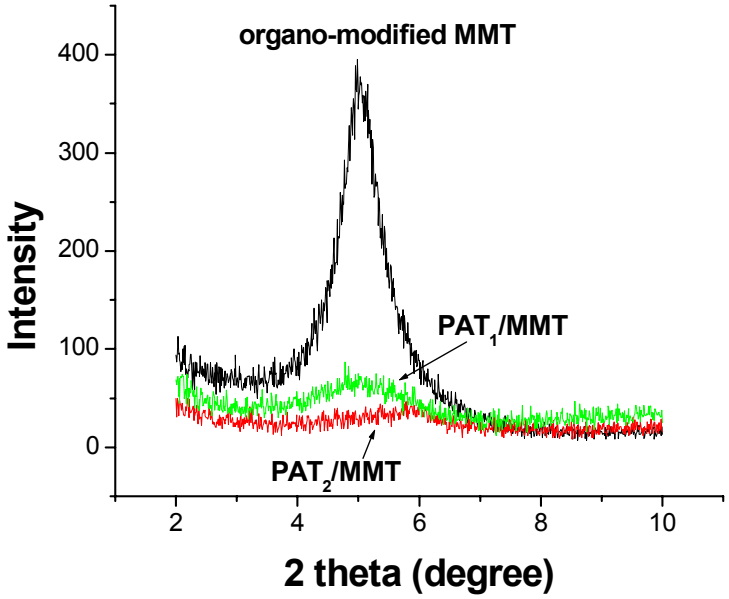

Fig. 3 – X-ray diffraction of modified MMT and the corresponding nanocomposites (PAT_1/MMT and PAT_2/MMT).

As can be seen from Fig. 3, the typical diffraction peak of PAT1/MMT nanocomposites is not shifted (2θ = 5°), but it has a lower intensity suggesting the formation of an intercalated nanocomposite with a lower degree of intercalation.[24] Usually, the intercalation of the polymer chains increases the interlayer spacing, in comparison with the spacing of the organo-modified clay. This can lead to a shift of the diffraction peak towards lower angle values. Probably, in our case the intercalated triazene polyacrylates chains peel the platelets away from the well-intercalated silicate stacks, a process followed by a decrease of intercalation.[25] For the second nanocomposite (PAT_2/MMT), the diffraction peak appeared as a weak shoulder at 2θ = 5.9° indicated the presence of clay as agglomerated sheets.[26]

FT-IR experiments were realized in order to provide information about the molecular structure of the materials and to study the microstructure changes of the triazene polyacrylates/ montmorillonite and pure montmorillonite. Fig. 4 shows the FT-IR spectra of modified montmorillonite and its nanocomposite samples recorded at room temperature.

We note that the above nanocomposites reveal the existence of some characteristic bands of the starting triazene polyacrylates (PAT_1 and PAT_2) centered at 2950 cm^{-1} (C-H) and 1352 cm^{-1} recognized for triazene units. The stretching vibration of the aromatic ring appears at 1598 cm^{-1}, 834 cm^{-1}(disubstituted aromatic ring for PAT_2) and 760 (monosubstituted aromatic ring for PAT_1) respectively, while the broad peak around 1720 cm^{-1} is assigned to the carbonyl group. As compared to the spectrum of modified MMT, the absorption band from 3638 cm^{-1} ascribed to –OH of MMT disappeared in the spectrum of triazene polyacrylates/MMT composites (PAT_1/MMT and PAT_2/MMT). Also, the absorption band at 1050 cm^{-1} attributed to the Si-OH of MMT shifted to 1145 cm^{-1} and its intensity decreased. These results indicate the participation of the –OH group of MMT in the formation of the hybrid nanocomposites based on triazene copolyacrylates.

Atomic Force Microscopy technique was used to characterize the morphology of triazene polyacrylates/MMT nanocomposites. Fig. 5 shows the AFM topographic and phase images of the triazene polyacrylates/clay composite films containing 3 wt. % MMT.

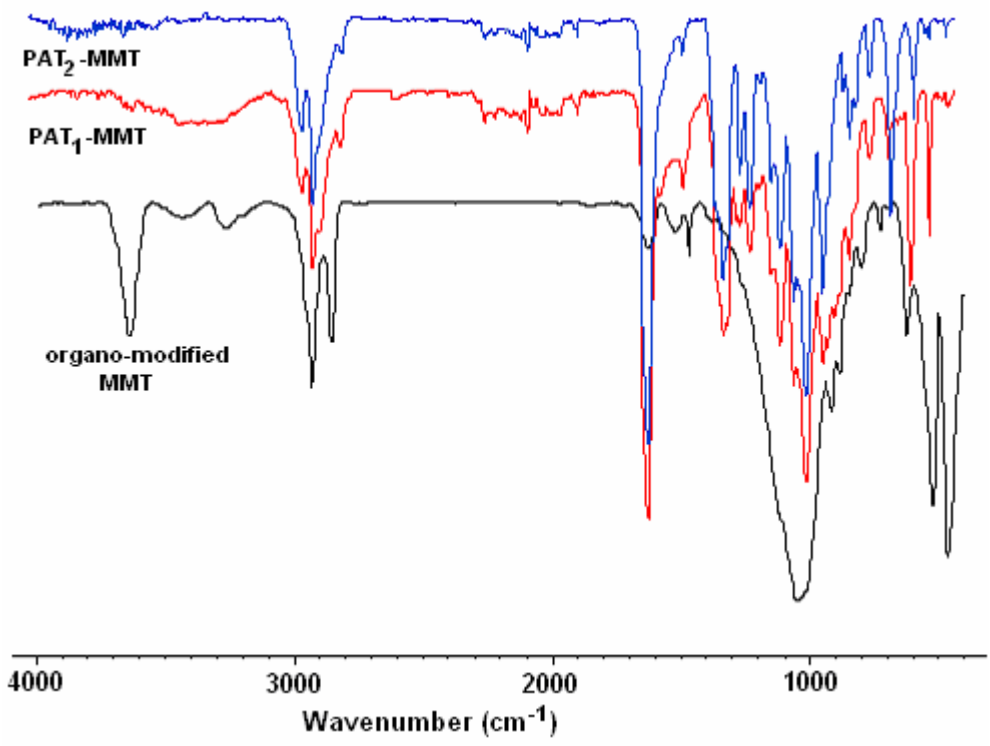

Fig. 4 – FT-IR spectra of organo-modified MMT and triazene polyacrylates/MMT composites.

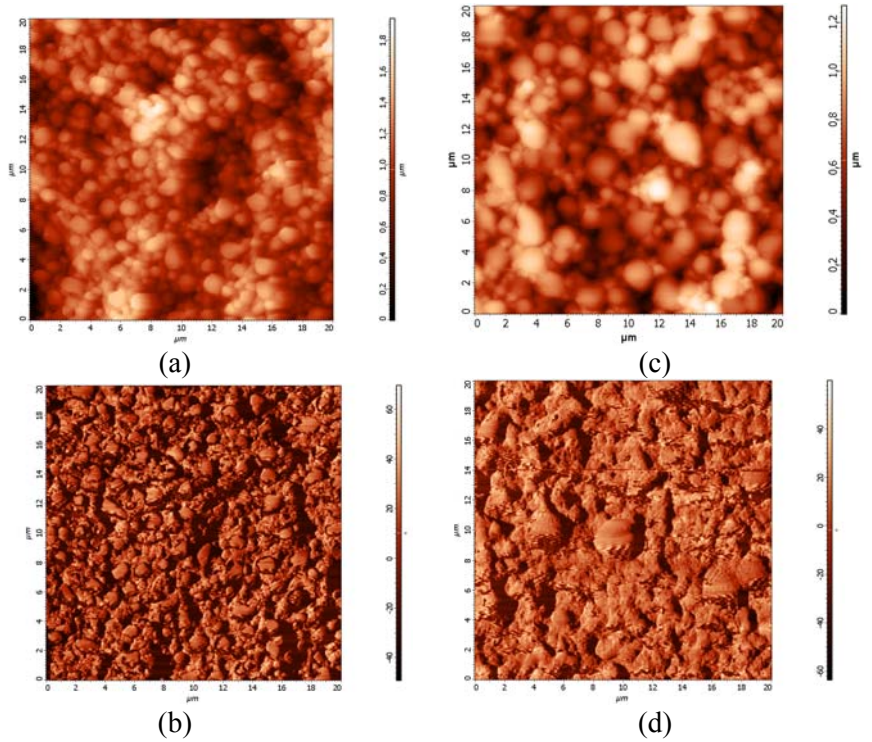

Fig. 5 – AFM topographic and phase images of PAT_1/MMT (a,b) and PAT_2/MMT (c,d) nanocomposites.

The appearance of topographic and phase images is quite similar, both images showing continuous global domains with bumpy areas. Moreover, the structural hierarchies of nanocomposite surface indicate adequate contrast between the inorganic MMT particles and the polyacrylates matrix; the brighter phase contrast and the darker areas in Fig. 5 (a) and (c)

correspond to the irregular granular MMT particles and polyacrylates matrix, respectively. It is also evident from the phase image of surface morphology that stacks of MMT are well dispersed in the skin layer of triazene polyacrylates matrix, according to XRD and SEM investigations. The mean surface roughness, R_a, of the samples was also measured. The R_a values are 111.927 nm for PAT_1/MMT and 132.471 nm for PAT_2/MMT nanocomposite, respectively.

SEM micrographs of the modified MMT (a) and polymeric nanocomposites (b and c) surface can be observed in figure 6. Nanocomposites films were frozen in liquid nitrogen, fractured and then examined.

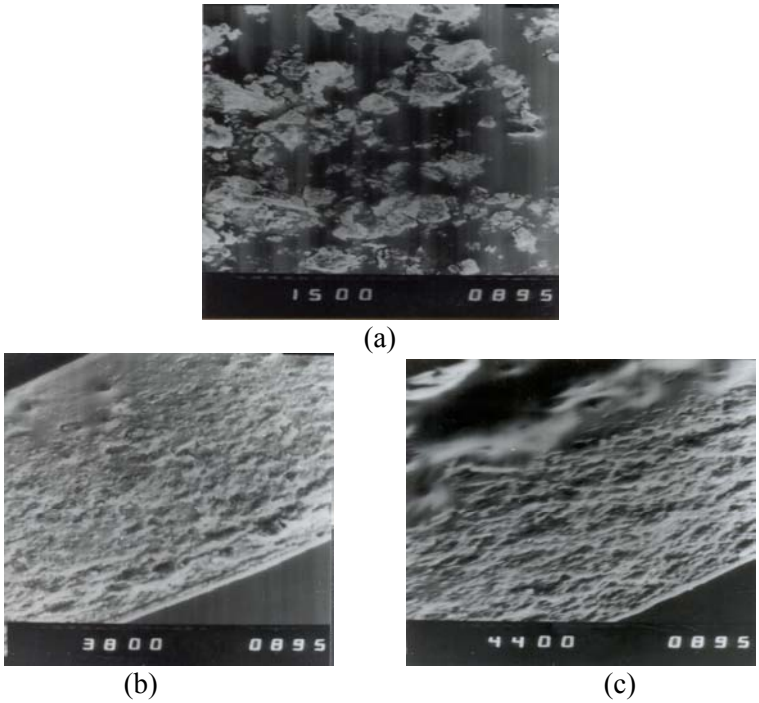

(a) (b) (c)

Fig. 6 – SEM images of (a) MMT and corresponding nanocomposites (b) for PAT_1/MMT and (c) for PAT_2/MMT.

Obviously, surface morphology of the nanocomposites is different from that of the starting MMT. No large aggregates and a homogenous distribution of the MMT in the polyacrylates matrix were observed in all triazene polyacrylates nanocomposites, implying good adhesion between organo-modified filler and matrix. It was proved, once again, the uniform distribution of the filler in the matrix, with important features for the improvement of the mechanical performance of the resulting nanocomposites.[27]

The thermal decomposition behavior of nanocomposite was investigated by thermogravimetric (TG) measurements. Table 2 and Fig. 7 (a) and (b) list the results of thermal stability for triazene polyacrylates nanocomposites (PAT_1 and PAT_2) prepared in this work.

According to Table 2 all samples present a three-step decomposition process, where the weight loss decomposition temperature of the starting polymers (PAT_1 and PAT_2) is about 90 °C (Fig. 7 (a) line 1) and 125 °C (Fig. 7 (b) line 1), respectively. When 3.0 wt. % of modified MMT was added, the decomposition temperature of composites raised at 115 °C (Fig. 7 (a) line 2) and 140 °C (Fig. 7 (b) line 2), correspondingly.

It seems that the first stage of the process is recognized as the decomposition of the triazene group from acrylic copolymer, when small volatile molecules, such as molecular nitrogen and aromatic compounds are released. The second stage is broad, in which the weight loss is ranging from 20 % to 70 % in the temperature range of 265–470 °C. At this level, the triazene polyacrylates nanocomposites composites displayed higher thermal resistance than pure polymers. Nanocomposites are almost completely decomposed above 650 °C and presents residue (not observed in the case of pure

polymers with triazene moieties). This stage and the next one were attributed to further decomposition of the polymer backbone. The improvement of thermal properties can be attributed to high thermal stability of clay and its interaction with macromolecular chains.

Table 2

Weight losses and decomposition temperatures of pure and triazene polyacrylates nanocomposites

Compound	Step of degradation	Temperature range (°C)	T_{max}(°C)	Weight loss (%)
PAT_1	I	90-161	121	13
	II	161-381	386	84
	III	381-500	470	100
	Residue 0 %			
PAT_1/MMT	I	115-230	185	12
	II	230-460	350	80
	III	460-650	570	95
	Residue 5 %			
PAT_2	I	125-265	200	11
	II	265-450	370	70
	III	450-680	600	99
	Residue 1 %			
PAT_2/MMT	I	140-265	210	20
	II	265-470	400	75
	III	470-720	650	95
	Residue 5 %			

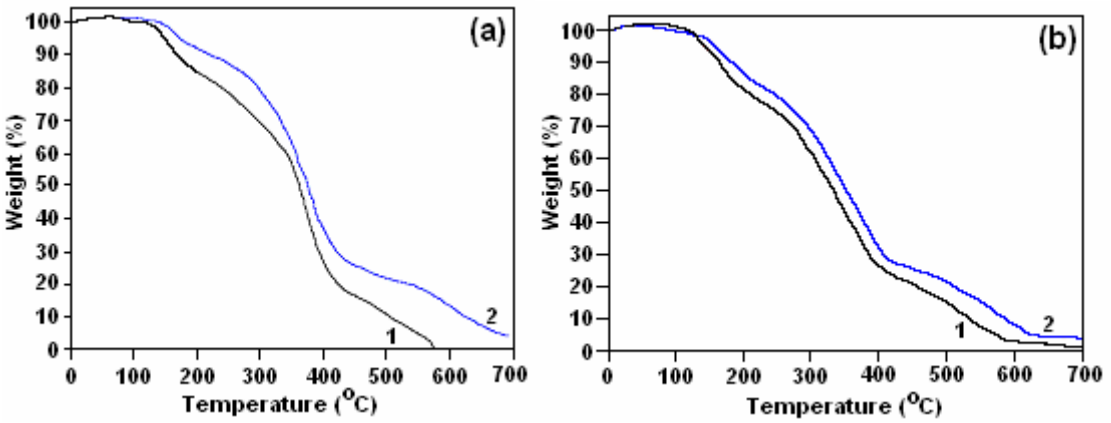

Fig. 7 – TGA curves of (a) PAT_1 (1); PAT_1/MMT (2); and (b) PAT_2 (1); PAT_2/MMT (2).

CONCLUSIONS

In this study, we synthesized two new triazene polyacrylates nanocomposites (**PAT_1/MMT** and **PAT_2/MMT**) using the solution-intercalation film-casting technique. The novel nanocomposite hybrid materials were characterized by X-ray, FT-IR, TGA and SEM techniques. The results clearly indicate that silicate layers are intercalated in the polyacrylate matrix and the thermal stability of the novel hybrid materials is higher compared to that of triazene polyacrylates with about 100 °C. This is a consequence of the favorable interactions between triazene polyacrylates and organo-modified silicate.

REFERENCES

1. Q.H. Zeng, A.B. Yu, G.Q. Lu and D.R. Paul, *J. Nanosci. Nanotech.*, **2005**, *5*, 1574-1592.
2. A. Usuki, Y. Kojima, M. Kawasumi, A. Okada, Y. Fukushima, T. Kurauchi and O. Kamigatio, *J. Mater. Res.,* **1993**, *8*, 1179-1184.
3. E. P. Giannelis, *Adv. Mater.,* **1996**, *8*, 29-35.
4. K. Yano, A. Usuki, T. Kurauchi and O. Kamigaito, *J. Polym. Sci. Part A: Polym. Chem.*, **1997**, *35*, 2289-2294.
5. T. Lan and T.J. Pinnavaia, *Chem. Mater.,* **1994**, *6*, 2216-2219.
6. P.B. Messersmith and E.P. Giannelis, *Chem. Mater.,* **1994**, *6*, 1719-1725.
7. Y. Kojima, A.Fujushima, A. Usuki, A.Okada and T.Kurauchi, *J. Mater. Sci. Lett.,* **1993**, *12*, 889-890.
8. Y. Kojima, A. Usuki, M.Kawasumi, T.Fukushima and O.Kamigaito, *J. Mater. Res.,* **1993**, *8*, 1179-1184.

9. T. Lan, P.D. Kaviratna and T.J. Pinnavaia, *Chem. Mater.,* **1994**, *6*, 573-575.
10. G. Ozin, *Adv. Mater.,* **1992**, *4*, 612-649.
11. J. Liu, Y. Gao, F. Wang, D. Li and J. Xu, *J. Mater. Sci.,* **2002**, *37*, 3085-3088.
12. V.E. Yudin, J. U. Otaigbe, S. Gladchenko, B.G. Olson, S. Nazarenko, E.N. Korytkova and V.V. Gusarov, *Polymer,* **2007**, *48*, 1306-1315.
13. H.B. Hsueh and C.Y. Chen, *Polymer,* **2003**, *44*, 1151-1161.
14. M. Kato, A. Usuki and A. Okada, *J. Appl. Polym. Sci.,* **1997**, *66*, 1781-1785.
15. A. Akelah and A. Moet, *J. Mater. Sci.,* **1996**, *31*, 1064-1066.
16. Z. Wang and T.J. Pinnavaia, *Chem. Mater.,* **1998**, *10*, 3769-3771.
17. W. Tao, F. Fei and W.Y. Chuan, *Polym. Bull*., **2006**, *56*, 413-426.
18. J. Zhang, K. Yuan, Y.P. Wang, S.J. Gu and S. Zhang, *Mater. Lett.,* **2007**, *61*, 316-320.
19. E.C. Buruiana, V. Melinte, T. Buruiana, T. Lippert, H. Yoshikawa and H. Mashuhara, *J. Photochem. Photobiol. A: Chem*., **2005**, *171*, 261-267.
20. E.C. Buruiana, V. Melinte, T. Buruiana, B.C. Simionescu, T. Lippert and L. Urech, *J. Photochem. Photobiol. A: Chem.,* **2007**, *186*, 270-277.
21. E.C. Buruiana, T. Buruiana, L. Hahui, T. Lippert, L. Urech and A.Wokaun, *J. Polym. Sci. Part A: Polym. Chem.,* **2006**, *44*, 5271-5282.
22. E.C. Buruiana, L. Hahui, T. Buruiana, L. Urech and T. Lippert, *J. Photochem. Photobiol. A: Chem.,* **2008**, *195*, 337-345.
23. D.S. Kim, J.T. Kim and W.B. Woo, *J. Appl. Polym. Sci.,* **2004**, *96*, 1641-1647.
24. H.R. Dennis, D. Chang, S. Kim, J.L. White, J.W. Cho and D.R. Paul, *Polymer,* **2001**, *42,* 9513-9522.
25. D.J. Voorn, W. Ming and A.M. van Herk, *Macromolecules,* **2006**, *39*, 4654-4656.
26. S. Kalambur and S.S.H. Rizvi, *J. Appl. Polym. Sci.,* **2005**, *96,* 1072-1082.
27. J. Zhang, L. Wang and A. Wang, *Ind. Eng. Chem. Res*., **2007**, *46*, 2497-2502.